NAVAL POSTGRADUATE SCHOOL
MONTEREY, CALIFORNIA

THESIS

MICROSTRUCTURE AND AGING RESPONSE OF SiC_p REINFORCED A356 Al METAL MATRIX COMPOSITE SUBJECT TO POST FABRICATION THERMOMECHANICAL PROCESSING

By
Donald Vincent Avenger
December 1994

Thesis Advisor: Indranath Dutta

REPORT DOCUMENTATION PAGE

Form Approved
OMB No. 0704-0188

1.AGENCY USE ONLY *(Leave blank)*	2.REPORT DATE	3.REPORT TYPE AND DATES COVERED
	DECEMBER 1994	Master's Thesis

4.TITLE AND SUBTITLE MICROSTRUCTURE AND AGING RESPONSE OF SiC_p REINFORCED A356 Al METAL MATRIX COMPOSITE SUBJECT TO POST FABRICATION THERMOMECHANICAL PROCESSING

5.FUNDING NUMBERS

6.AUTHOR(S)
Avenger, Donald V.

7.PERFORMING ORGANIZATION NAME(S) AND ADDRESS(ES)
Naval Postgraduate School
Monterey CA 93943-5000

8.PERFORMING ORGANIZATION REPORT NUMBER

9.SPONSORING/MONITORING AGENCY NAME(S) AND ADDRESS(ES)

10.SPONSORING/MONITORING AGENCY REPORT NUMBER

11.SUPPLEMENTARY NOTES The views expressed in this thesis are those of the author and do not reflect the official policy or position of the Department of Defense or the U.S. Government.

12a.DISTRIBUTION/AVAILABILITY STATEMENT
Approved for public release; distribution is unlimited.

12b.DISTRIBUTION CODE

13.ABSTRACT *(maximum 200 words)*

The microstructure and aging behavior of a centrifugally cast A356 Al-SiC_p metal matrix composite was studied as a function of post-fabrication processing via transmission electron microscopy (TEM) and differential scanning caloritemtry (DSC). The effects of total rolling strain, strain per rolling pass and rolling temperature on both microstructure and precipitation behavior were investigated. It was found that post-fabrication processing had relatively little effect on the kinetics of the various precipitation processes that constitute aging, although they affected the amounts of the various precipitates significantly.

14. SUBJECT TERMS Aluminum composites, Metal Matrix composites, Aluminum Castings, Fibre Reinforced Auminum Castings, Silicon Carbide

15.NUMBER OF PAGES 46

16.PRICE CODE

17. SECURITY CLASSIFICATION OF REPORT	18. SECURITY CLASSIFICATION OF THIS PAGE	19.SECURITY CLASSIFICATION OF ABSTRACT	20.LIMITATION OF ABSTRACT
Unclassified	Unclassified	Unclassified	UL

NSN 7540-01-280-5500

Standard Form 298 (Rev. 2-89)
Prescribed by ANSI Std. 239-18
298-102

Approved for public release; distribution is unlimited.

MICROSTRUCTURE AND AGING RESPONSE OF SiCp REINFORCED
A356 Al METAL MATRIX COMPOSITE
SUBJECT TO POST FABRICATION
THERMOMECHANICAL PROCESSING

by

Donald V. Avenger
Lieutenant, United States Navy
B.S.Met. E., Ohio State University, 1984

Submitted in partial fulfillment of the
requirements for the degree of

MASTER OF SCIENCE IN MECHANICAL ENGINEERING

from the

NAVAL POSTGRADUATE SCHOOL
December 1994

Author: Donald V. Avenger
Donald V. Avenger

Approved by: Indranath Dutta
Indranath Dutta, Thesis Advisor

Mathew D. Kelleher
Mathew D. Kelleher, Chairman,
Department of Mechanical Engineering

ABSTRACT

The microstructure and aging behavior of a centrifugally cast A356 Al-SiC_p metal matrix composite was studied as a function of post-fabrication processing via transmission electron microscopy (TEM) and differential scanning calorimetry (DSC). The effects of total rolling strain, strain per rolling pass and rolling temperature on both microstructure and precipitation behavior were investigated. It was found that post-fabrication processing had relatively little effect on the kinetics of the various precipitation processes that constitute aging although they affected the amounts of the various precipitates significantly.

TABLE OF CONTENTS

I. INTRODUCTION **1**
- A. METAL MATRIX COMPOSITES 1
- B. THERMOMECHANICAL PROCESSING OF A CAST MMC 2
- C. EFFECT OF TMP ON AGING IN A356 SILICON CARBIDE PARTICLE REINFORCED ALUMINUM ALLOY 3

II. RESEARCH OBJECTIVE **7**

III. DESCRIPTION OF MATERIALS **9**

IV. EXPERIMENTAL PROCEDURE **11**
- A. THERMOMECHANICAL PROCESSING 11
- B. DIFFERENTIAL SCANNING CALORIMETRY 11
- C. HARDNESS TESTING 13
- D. TRANSMISSION ELECTRON MICROSCOPY 14

V. RESULTS AND DISCUSSION **17**
- A. EFFECT OF PARTICULATE ADDITION TO MATRIX AGING RESPONSE 17
- B. EFFECT OF STRAIN PER ROLLING PASS 17
- C. EFFECT OF ROLLING TEMPERATURE 23
- D. EFFECT OF TOTAL ROLLING STRAIN 27

VI. CONCLUSIONS **33**

REFERENCES **35**

INITIAL DISTRIBUTION LIST **37**

I. INTRODUCTION

A. METAL MATRIX COMPOSITES

As the continuing quest for light weight, strong yet ductile materials drives investigations into exotic metal alloys, one relatively uncomplicated, commercially viable market of materials has not yet been fully exploited. Metal matrix composites (MMC) can fill the void for ease of production, large part size and consistent mechanical properties. To date, the widespread use of composite alloys in engineering applications is limited by cost of fabrication, limited part size and other restrictive characteristics. Powder metallurgy processes where the particle reinforcement and a powdered metal matrix are mixed and compressed under elevated temperatures and pressures is a case in point.

Casting techniques used with ceramic reinforced castable alloys may relieve the restrictions in high cost and low product size. In fact, taking advantage of known casting practices has resulted in a cost-effective way to benefit from the improved mechanical properties of metals reinforced with ceramic fibers, whiskers, or particles. Recently, the centrifugal casting process has been adapted successfully by researchers at NSWC, White Oak for producing high volume MMC parts with rotational symmetry at large production rates [Ref. 1]. The process begins by injecting a premixed ceramic reinforced metal melt into a heated cylindrical permanent mold spinning at high rpm. On contact with the rotating mold, solidification begins at the mold wall and proceeds through the thickness of the melt until a solid part with cylindrical symmetry is produced. During solidification, any difference in densities between the particulates and the

melt may result in segregation of the particles in the solid, usually in the form of a through-thickness gradient. This typically results in a particulate volume fraction that varies through the thickness of the casting, the highest being significantly larger than the nominal reinforcement volume fraction in the melt. In addition to this macroscopic segregation, clusters of particles may occur on a microscopic scale due to surface tension effects and voids may form inside clusters [Ref. 2, 3]. Such clustering and voids are known to produce poor ductility in cast MMCs. On the positive side, the relatively rapid cooling rate during centrifugal casting makes it possible to eliminate the dendritic structure of the as cast Al-Si eutectic alloy that is unfavorable to reliable mechanical properties [Ref. 4]. Also, a rapid cooling rate promotes a more homogeneous distribution of SiC particles which results in higher as cast strength parameters [Ref. 5, 8]. Ultimately, however, as in any other casting process for MMCs, the mechanical properties of the as-centrifugally cast MMCs must be improved in order to make it more commercially competitive.

B. THERMOMECHANICAL PROCESSING OF A CAST MMC

In cast MMCs persistent problems of poor wetting of the reinforcement by molten metal and inhomogeneous reinforcement distribution due to flocculation result in poor as-cast microstructures and properties [Ref. 21]. Thermomechanical processing (TMP) such as hot isostatic pressing (HIPing), extrusion or rolling is employed to improve the microstructure and hence the mechanical properties. In general, the metal matrix microstructure is improved through the elimination of micropores and interparticle voids and redistribution of reinforcement particles.

Sufficient mechanical processing is required to break down the as-cast microstructure and impart ductility and toughness through homogenization. Past

studies [Refs. 6, 7, 18] have established that TMP can significantly improve the mechanical properties of cast MMCs. It was found that material ductility was improved when TMP was employed to more homogeneously distribute the ceramic particles and, hence, lessen the degree of localized deformation. Additionally, appropriate TMP may induce a very fine grain and subgrain structure. This can be attributed either to particle stimulated nucleation (PSN) of small matrix grains at particle-matrix interfaces [Ref. 6], or the dynamic recrystallization of the matrix during TMP as dislocations continuously recover at grain or subgrain boundaries, eventually converting them to high angle boundaries [Ref. 7]. McNelley *et al.*[Ref. 21] subjected an Al-10 Mg-0.1 Zr nonreinforced alloy to TMP consisting of rolling at 300°C which included a 30 minute interpass anneal (IPA) time also at 300°C. Superplastic elongations at 300°C exceeding 1000% was attributed to PSN of recrystallization and its associated grain refinement. In composites, such PSN may be utilized to obtain enhanced ductilities and toughnesses via TMP.

C. EFFECT OF TMP ON AGING IN A356 SILICON CARBIDE PARTICLE REINFORCED ALUMINUM ALLOY

The effect of the addition of ceramic particles to the aging response of age hardenable aluminum alloys has been documented in several studies [Ref 4, 9-13]. Experimental evidence indicates that the addition of SiC particulates to aluminum does not qualitatively alter the sequence by which precipitation hardening occurs. However, it has been observed that the aging kinetics, as well as the amounts of different precipitate phases in the composites are altered relative to the unreinforced alloy [Ref. 11]. The addition of reinforcement affects both nucleation and growth rates of the metastable transition phases. Generally it

is agreed that the accelerated aging of the composites is due to an increase in matrix dislocation density that arises form a coefficient of thermal expansion (CTE) mismatch between the SiC particles and the Al matrix. On quenching from the solutionizing temperature a large plastic strain is originated between matrix and particle resulting in a large increase in the dislocation density as observed by transmission electron microscopy (TEM) [Ref 11]. This increase significantly enhances the diffusivity of Mg in aluminum via dislocation pipe diffusion and hence accelerates precipitation of the transition phase. In addition to accelerated growth of the precipitating phases, nucleation of the transition phase is also accelerated as the large number of dislocations produced due to CTE mismatch provides numerous sites for heterogeneous nucleation of transition precipitates, reducing the incubation time for nucleation.

It is also worthwhile to note that a recent study on a precipitation hardenable aluminum alloy reinforced with SiC concluded that materials fabricated by different techniques, i.e., squeeze casting or powder metallurgy, did not show significant differences in their aging kinetics [Ref. 14].

While the aging kinetics of a reinforced alloy as compared to its unreinforced counterpart has been documented, little work has been done on the relative effects of various TMP on a reinforced hardenable alloy. In a study by May [Ref. 12], it was found that an A356 SiC particle reinforced alloy that had been extruded (3.5:1.0 reduction) ages more slowly than its as-cast counterpart. Additionally, the formation of the primary hardening constituents was also delayed. This was attributed to recovery of interfacial dislocation to the grain/subgrain boundaries, decreasing the density of random dislocation available for precipitation within subgrains. May also correlated this decelerating trend in

the precipitation of hardening constituents through microhardness data. There, he found that the effects of extrusion affected the monolith and composite differently; extrusion accelerated aging in the monolith while delaying it slightly in the composite. He attributed the delay in peak hardness of the extruded MMC also to the recovery of dislocations generated due to the CTE mismatch to grain/subgrain boundaries.

(blank)

II. RESEARCH OBJECTIVE

The study on the effect of the addition of SiC particulates to aluminum alloys has received considerable attention recently. Qualitatively, the precipitation sequence in aluminum alloys is not altered by the addition of particulate. However, aging kinetics have been found to be altered as composites usually age significantly faster than the monolithic alloy.

Most studies have dealt strictly with the comparison of unreinforced to reinforced alloy and are generally centered around wrought alloys. Little systematic study has been directed to reinforced castable alloys and factors that can affect their mechanical properties. More specifically, little has been directed toward post fabrication TMP on particle reinforced cast aluminum alloys. McNelley and Kalu [Ref. 7] demonstrated an increase in strength and ductility with specific thermomechanical treatments on 6061 Al-Al_2O_3 composite, Dutta *et al.* [Ref. 18] showed an increase in both strength and ductility with increasing TMP in a commercially cast aluminum alloy 5083 reinforced with 10 volume percent SiC particles, and Cottu *et al.* [Ref. 4] showed that the precipitate phase coarsened if the alloy is strained at elevated temperature in a SiC fiber reinforced AS7G05 aluminum alloy.

The purpose of the present work is two fold. The first objective is to characterize the aging behavior of an A356 particle composite alloy as a function of TMP condition and compare the results with that obtained by May [Ref. 12] on the same alloy reinforced with 26 volume percent SiC particles that had been either HIPed (670K, 30 ksi, 2 hrs) or co-extruded. The second objective is to conduct a TEM investigation of the microstructural evolution of the same alloy as

a function of TMP schedules. The TMP parameters varied in this study are rolling temperature, amount of strain per rolling pass and total rolling strain.

III. DESCRIPTION OF MATERIALS

The composite material used in this study, A356 reinforced with 19 volume percent SiC particles, was received from the Naval Surface Warfare Center, White Oak. This material was centrifugally cast as previously described using a patented process [Ref. 1]. The control monolithic material was a commercial grade A356 Al alloy also centrifugally cast at the Naval Surface Warfare Center. The nominal composition of A356 is presented in Table 1. [Ref. 17]

Si	Mg	Cu	Fe	Ti	Mn	Zn	rest
6.5	0.45	0.20	0.20	0.20	0.10	0.10	0.15
to	to	max	max	max	max	max	max
7.5	0.25						total

Table 1. Composition of A356 aluminum.

The as-cast composite, which constituted a cylindrical shell, was flattened by hot-processing at 520°C into bars 228.6 mm (9 inches) long by 50.8 mm (2 inches) wide and 25.4 mm (1 inch) thick. Because of segregation of the SiC particles to the outside walls of the mold during centrifugal casting, the bars revealed a light gray color on the inner diameter with a darker gray color on the outside diameter. The darker, outside diameter material was determined through image analysis to contain 19 volume percent SiC particles while the inside diameter was monolithic [Ref. 20]. The inside, monolithic layer was removed by diamond saw so that studies could be centered strictly on the composite.

The composite was then rolled at nominal reductions of either five or ten percent per pass. Prior to rolling, and between rolling passes, the samples were

soaked at temperatures of either 400°C, 480°C, or 545°C for 45 minutes. Following TMP, the samples were mechanically tested in the solutionized and quenched state [Ref. 20]. Samples used for DSC and TEM analysis were cut from the butt end of tensile coupons that had been previously cut and pulled.

IV. EXPERIMENTAL PROCEDURE

A. THERMOMECHANICAL PROCESSING

The material used for the generation of DSC thermograms and TEM micrographs was cut from the butt end of tensile coupons used in a previous study [Ref. 20]. A synopsis of the TMP given to those tensile bars is appropriate.

All as-cast material underwent an eight hour homogenization heat treatment at 540°C prior to processing. To flatten the as-cast material it was forged at 520°C at a forging pressure low enough to maintain dimensional integrity. The material was then thermomechanically processed by rolling with soaking times of 45 minutes between each pass. Three temperatures were used during the rolling process; 400°C, 480°C and 545°C. The lower temperature is significantly below the solvus temperature, the 480°C temperature is very near yet below the solvus line and the upper temperature is slightly above the homogenization curve. Two strain rates of five or ten percent deformation per rolling pass were used with mill deflection taken into account. Table 2 summarizes the TMP given to each sample used in this study. The nomenclature is that which was assigned by Muller and used during the present study to retain continuity. The strain percentages listed are true strain.

B. DIFFERENTIAL SCANNING CALORIMETRY

A Perkin Elmer Model 7 Differential Scanning Calorimeter (DSC) was used to monitor and record the solid state phase transitions occurring in the test alloy. Five millimeter discs were cut from the butt end of tensile bars with a Servomet spark machine. The samples were then hand sanded on 340 grit paper to a

weight of approximately 46 mg (0.5-1.0 mm in thickness). An analytical scale was used to weigh the samples. The disc-shaped samples were wrapped in aluminum foil and solutionized in a Marshall Model 1134 horizontal tube furnace controlled by a Eurotherm Model 808 controller at 540°C. Argon gas was used to prevent oxidation. The samples were solutionized for 90 minutes followed by a vigorous ice water quench.

	total strain (%)	rolling temp (°C)	stain per pass (%)
K-10-2	27.6	545	10
K-10-3	27.3	545	5
K-10-4	24.6	400	10
K-10-5	25.9	480	10
K-10-6	53	400	10
w-1-1	0	-	-

Table 2. TMP schedules for given sample nomenclature.

Immediately upon quenching the samples were dried, encapsulated in a sample pan and placed in the left hand chamber of the DSC. The time interval from ice bath to DSC chamber was on average two minutes. Pure aluminum of approximately the same weight as the sample was placed in a sample pan and used as a reference in the DSC's right hand chamber. A baseline was run using empty sample pans in each chamber each day before any samples were scanned. The baseline was used and subtracted from each run. All tests were run with the following parameters:

- Lower Temperature: 313 K
- Upper Temperature: 833 K

- Scan Rate: 10 K / minute
- Nitrogen gas flow rate: 1 bubble per second (monitored from exhaust port)

Several samples of each processed condition were scanned to ensure reproducibility of results. After a scan was completed, the heat flow versus temperature data was converted to heat capacity versus temperature using the following equation:

$$\frac{\text{Heatflow(W)}}{\text{Scanrate}\left(\frac{\text{K}}{\text{s}}\right)} \times \frac{1}{\text{moles Al}} = \Delta C_p \left(\frac{\text{J}}{\text{K·mole}}\right) \qquad (1)$$

Moles of aluminum was obtained by first converting the volume fraction of the SiC particles to weight fraction of SiC as:

$$\rho_{composite} = (\rho_m V_m + \rho_p V_p) / V_{composite} \qquad (2)$$

$$\rho_{composite} = \rho_m \vartheta_m + \rho_p \vartheta_p \qquad (3)$$

$$\text{wt. fraction of SiC} = \vartheta_p \rho_p / \rho_c \qquad (4)$$

Weight of aluminum in the sample was then calculated as:

$$\text{wt. of Al} = \text{wt. of MMC sample} \times (1\text{-wt. fraction of SiC}) \qquad (5)$$

The data from all material runs were normalized by mass of the aluminum alloy.

C. HARDNESS TESTING

Hardness samples were wrapped in aluminum foil then solutionized in a Marshall Model 1134 horizontal tube funace with a Eurotherm Model 808 controller at 540°C. Argon gas was used to prevent oxidation. The samples were homogenized for ninety minutes then vigorously quenched in ice water.

The samples were then aged in a Blue-M furnace Model B-2730Q at a temperature of 155°C. The samples were put on an aluminum plate with the plate temperature being monitored with an Omega microcomputer thermometer Model

DP703. After aging, the samples were quenched in ice water, then tested for hardness. Hardness testing was conducted using a Rockwell Hardness Tester Model 1 JR. A 1/16 inch diameter ball was used with a 100 kg mass for the Rockwell B scale. The hardness of each sample was tested ten times then averaged [Ref. 20].

D. TRANSMISSION ELECTRON MICROSCOPY

The preparation of samples for viewing under the TEM is made difficult by the presence of the hard SiC particles within a relatively soft aluminum matrix. The SiC particles hinders the ability to obtain large regions of thin metal matrix which prompted a slight modification of typical ion milling procedure.

Again using the butt end of the tensile coupons, very thin wafers of the composite were cut using a high concentration diamond wheel and a Buehler Isomet 11-1180 low speed saw. The wafers were mounted on to a steel plug with thermal wax and hand reduced on emery paper through the normal succession of 240 to 600 grit paper. Reduction was ceased when it was certain the wafer was less than 100mm in thickness. Carefully lifting the thin sample from the plug by first heating, 3mm diameter disks were punched and placed in a TEM sample holder. Individual samples were dimpled on a Gatan model 656 dimple grinder by the method of setting the final thickness. 3 micron alumina paste was used a the abrasive medium. A final thickness setting of 35 mm produced consistent results.

Dimpled samples were solution and quenched in the same manner as the DSC samples and then immediately aged at 155°C for 700 minutes in the left hand chamber of the DSC 7. The 700 minute age time was determined to be the time to peak age as established via an aging curve generated from samples of the composite that had been rolled to 24.6% reduction at 400°C, Figure 1 pertains.

Upon aging all samples were quenched in ice water. Any storage after this point was in a freezer. The samples were further prepared with a Gatan model 600 duo ion-miller, on a cold stage cooled with liquid nitrogen. The accelerating voltage was 7 kV and the gun current was 1 mA. The specimens were milled for the first five hours at a gun angle of 13 degrees and then for the remainder of the mill time with the gun set at 12.5 degrees. This strategy was established to help maximize the amount of thin metal matrix area and minimize ion damage. Typical milling time was 9 hours per sample. TEM observation was performed on a JEOL 100 CX TEM at an accelerating voltage of 120 kV.

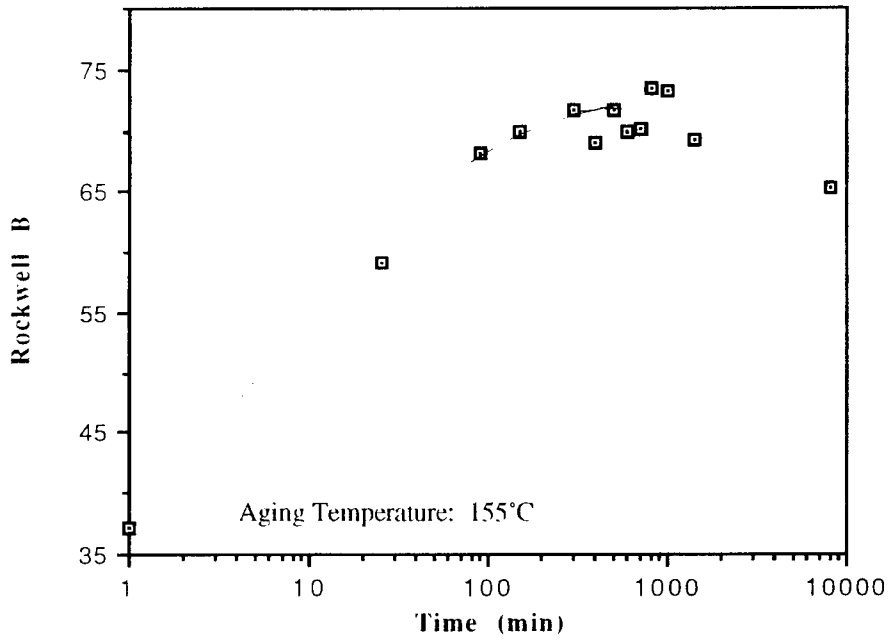

Figure 1. Aging data for A356 SiC_p rolled to 24.5% reduction at 400°C.

(blank)

V. RESULTS AND DISCUSSION

A. EFFECT OF PARTICULATE ADDITION TO MATRIX AGING RESPONSE

In comparing the DSC thermograms of the as-cast MMC to the monolithic alloy in Figure 2, two features are apparent. Both the β″ and β′ transformations are accelerated in the MMC and the relative volume fractions of both metastable phases are reduced. The peak temperatures of each exotherm is listed in Table 3. As previously rationalized [Ref. 11], the increased dislocation density of the MMC due to CTE mismatch of the SiC particles and Al matrix provides for increased number of heterogeneous nucleation sites, decreased incubation time and increased nucleation rate of the metastable transition phase. Diffusion is also aided by dislocation pipes, accelerating aging times in the MMCs. The reduced volume fraction of the transition phases is attributed to decreased vacancy concentration in the MMCs.

B. EFFECT OF STRAIN PER ROLLING PASS

Figure 3 shows the DSC thermograms of the MMC subject to 27.3% reduction at 545°C and 5% reduction per pass and the MMC subject to 27.6% reduction at 545°C and 10% reduction per pass both after solutionizing and quenching. Three distinct exothermic peaks are visible. The first exothermic peak represents the formation of the metastable β″ phase, the second represents

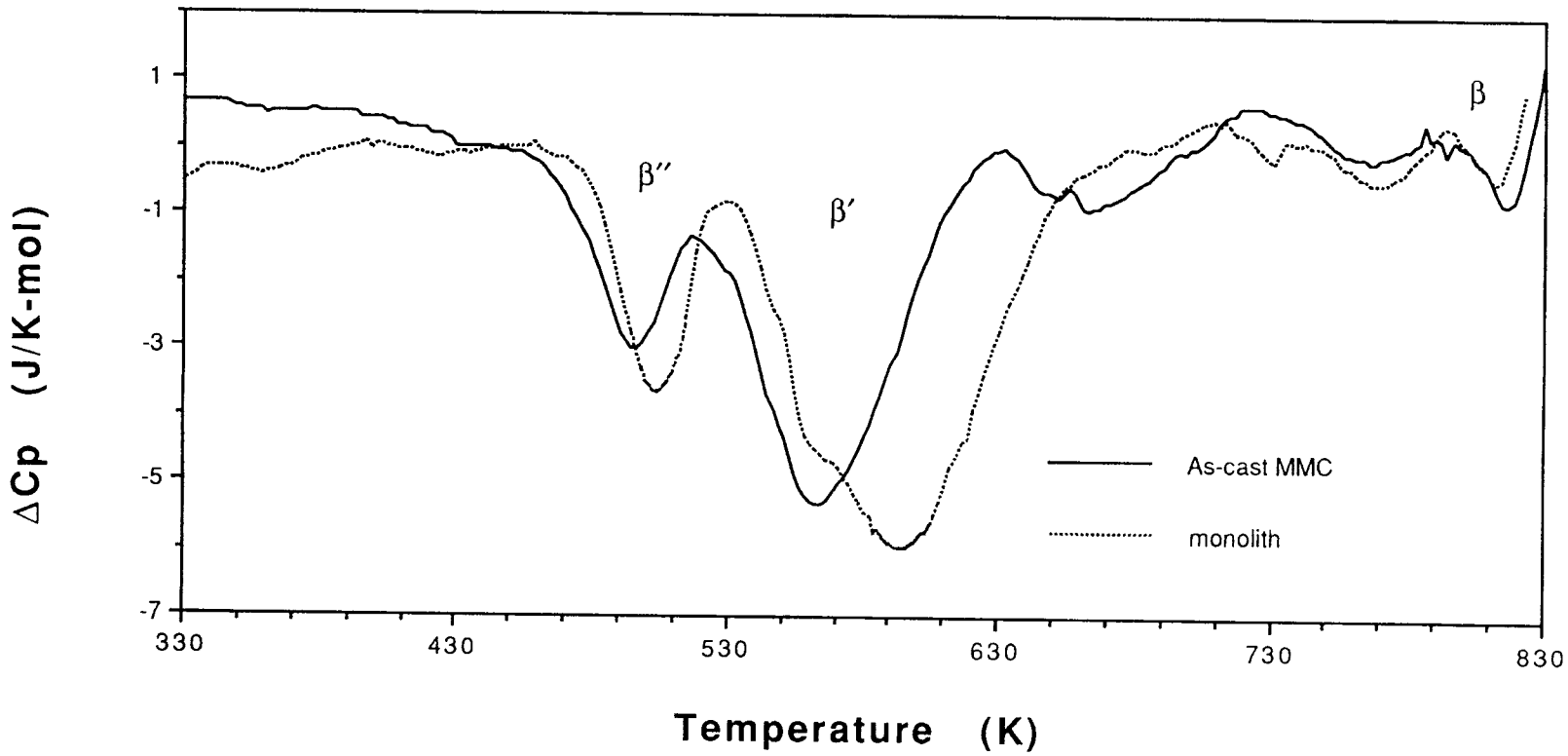

Figure 2. DSC thermograms of as-cast MMC and monolithic A356 Al alloy.

	As Cast MMC	Monolith
Peak	Temp (K)	Temp (K)
β''	496.35	504
β'	536.35	595
β	543	814

Table 3. Exotherm peak temperatures, as-cast MMC and monolithic A356 Al alloy.

the formation of the β′ phase and the third set of exothermic peaks represents the formation of the equilibrium β platelets [Ref. 16]. The peak temperatures of the β″, β′ and β peaks are listed in Table 4.

Several effects of this TMP schedule are evident. First, the β″ peak associated with the MMC rolled at 5% per pass is slightly accelerated relative to the MMC rolled at 10% per pass. The peak representing β′ and β phase show no significant shift in temperature suggesting that the kinetics of the precipitation of these two phases are not altered by TMP. Second, by comparing the relative sizes of the peaks which is proportional to the volume fraction of each precipitate formed, the MMC rolled at 5% per pass shows a greater amount of β″ and β′ relative to the MMC rolled at 10% per pass.

TEM characterizations of the resultant microstructure are represented in Figures 4 and 5 for the MMC rolled at 5% and 10 % per pass respectively. Examination by TEM of the MMC rolled to 27.3% reduction at 545°C and 5% per pass (Figures 4a and 4b), revealed a recovered microstructure with a clearly defined subgrain structure. Subgrains showed low misorientations with widely spaced dislocations clearly visible in the subgrain boundaries. The subgrains themselves contained numerous dislocations. The microstructure of the MMC rolled at 10% per pass is shown in Figure 5. Here, the subgrain boundaries did not show resolvable dislocations suggesting that recrystallization has probably occurred. The average subgrain size was comparable to the 5% per pass sample, as was the overall density of dislocations, suggesting that the subgrain boundaries have turned into high angle boundaries via absorption of dislocation during TMP (i.e., dynamic recrystallization).

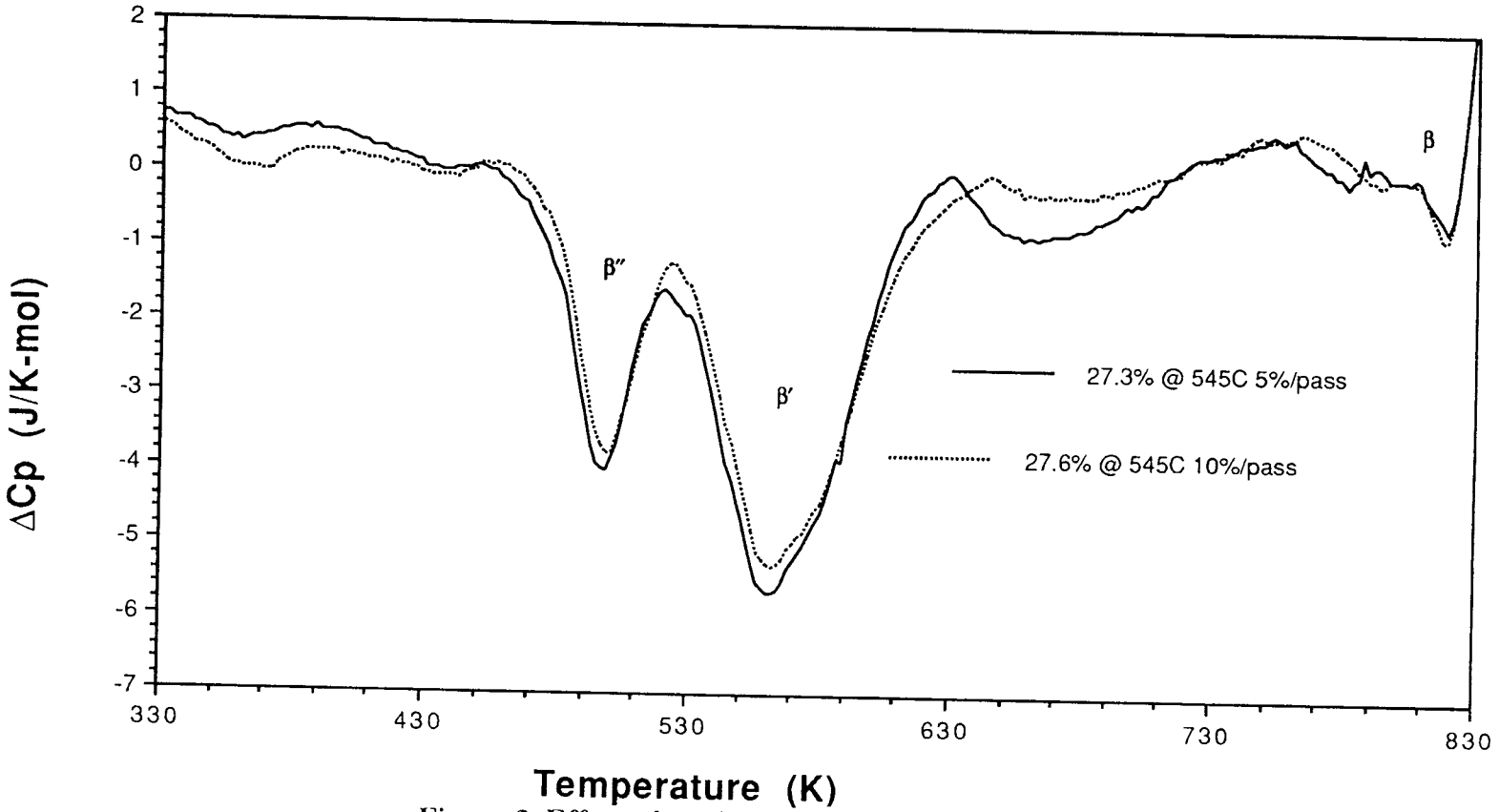

Figure 3. Effect of strain per pass in SiC_p A356 Al at 545°C.

	24.3% @ 545C 5%/p	27.6% @ 545C 10%/p
Peak	Temp (K)	Temp (K)
β″	498	499.15
β′	562.15	562.65
β	819	819

Table 4. Exotherm peak temperatures, effect of strain per pass in SiC_p A356 Al at 545°C.

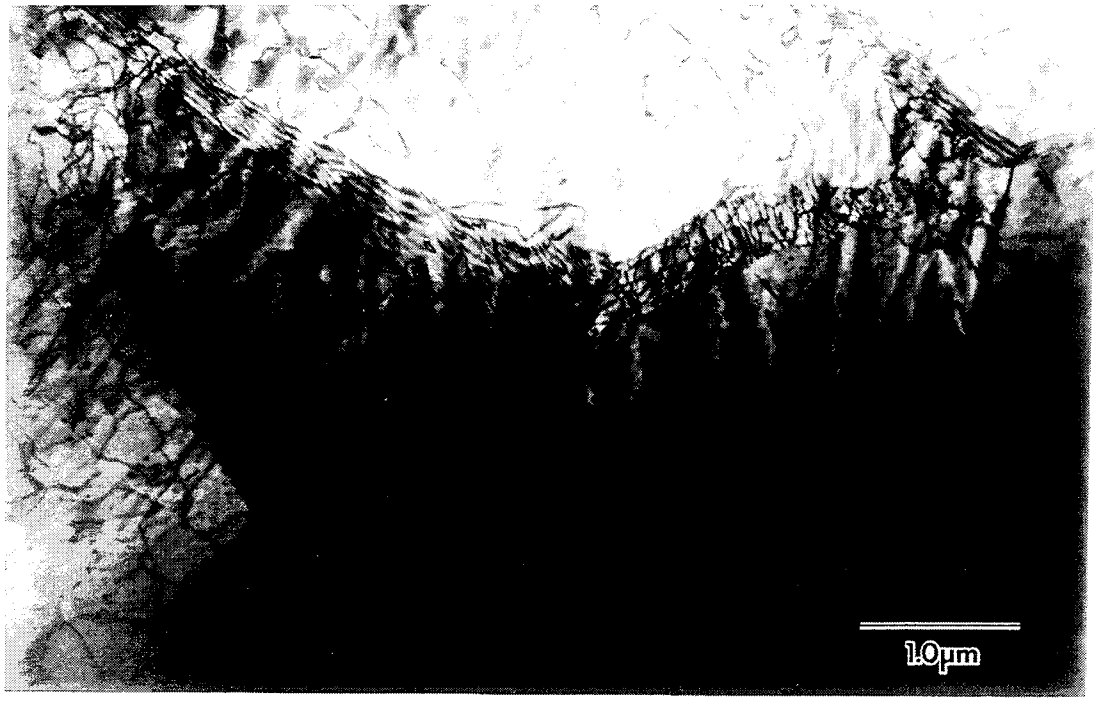

(a)

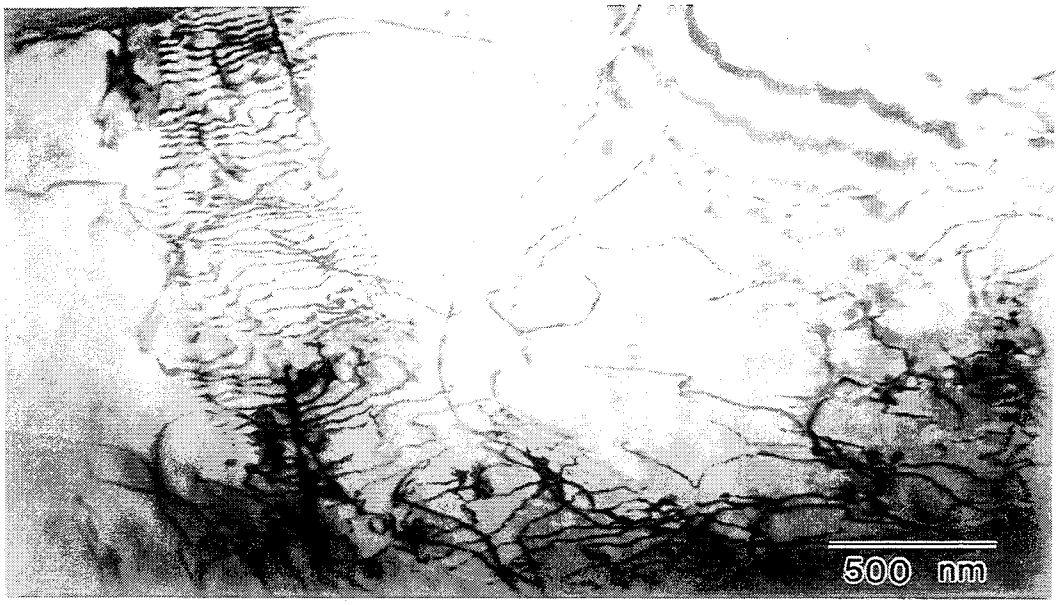

(b)

Figure 4. TEM micrographs of MMC strained to 27.3% at 545°C and 5% per pass. Recovered subgrain structure in vicinity of SiC particle (a). Close up of subgrain boundary (b).

Figure 5. TEM micrograph of MMC strained 27.6% at 545°C and 10 % per rolling pass.

The occurrence of dynamic recrystallization in the MMC rolled at 10% per pass affects the overall vacancy concentration within subgrains. The more clearly defined and generally higher angle boundaries of the recrystallized microstructure act as a more efficient sink for vacancies than the lower angle boundaries observed in the MMC rolled at 5% per pass. This, coupled with the observation that the dislocation densities within subgrains are nearly equal between the 10% and 5% per pass sample (dislocations are weaker vacancy sinks than grain boundaries), leads to the conclusion that the overall vacancy concentration is less for the 10% per pass sample relative to the 5% per pass sample. As the β″ phase precipitates at quenched-in vacancies, [Ref. 11] a higher nucleation rate is expected for the MMC with the higher vacancy concentration. Additionally, the higher vacancy concentration will aid growth of this phase by enhancing

diffusion of Mg through the matrix. The DSC thermogram in Figure 3 shows that the sample with higher vacancy concentration, i.e., the 5% per pass sample, contains more β″ phase relative to the 10% per pass sample as well as slightly accelerated transformation kinetics of the β″ phase.

The higher vacancy concentration for the sample rolled at 5% per pass also affects the relative amount of β′ phase. As the β′ phase nucleates at dislocations [Ref. 11], growth is enhanced by vacancy concentration and hence the 5% per pass sample shows a greater volume fraction of β′ precipitate relative to the 10% per pass MMC. Also noted from Figure 3 is the absence of any relative acceleration of the β′ phase in the 5% per pass MMC. The presence of subgrain boundary dislocations could be expected to accelerate nucleation of β′. Perhaps this is not observed because the random dislocation density inside the subgrains is not significantly higher in the 5% per pass sample than in the 10% per pass sample, the majority of the dislocations being arranged in low angle boundaries. Within the subgrain boundaries, the nucleation rate of β′ will be high, but the growth rate may not be very high, since the local concentration of vacancies may be low in the boundary. The eventual growth rate is likely to be determined by the competition of vacancy aided lattice diffusion and dislocation pipe diffusion in the boundary, and may not be significantly higher than that in the 10% per pass sample, where the higher angle grain boundaries can also act as effective nucleation sites and growth paths.

C. EFFECT OF ROLLING TEMPERATURE

The effect of rolling temperature on the aging response of A356 SiC_p is illustrated in Figure 6. Table 5 catalogs the peak temperature associated with Figure 6. Three separate samples were reduced at 10% per rolling pass to nearly

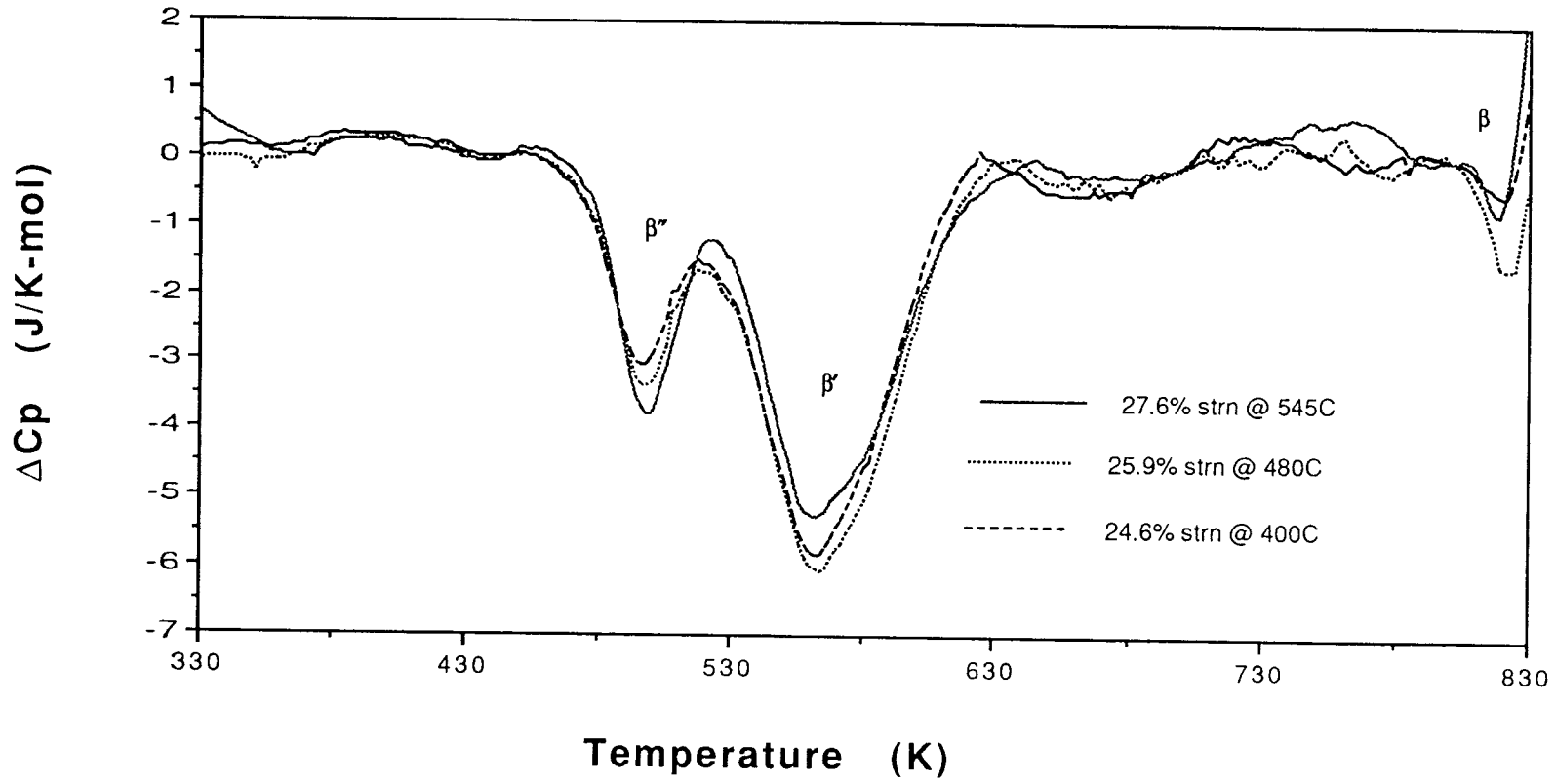

Figure 6. Effect of rolling temperature in SiC_p A356 Al.

	27.6% @ 545C	25.9% @ 480C	24.6% @ 400C
Peak	Temp (K)	Temp (K)	Temp (K)
b"	499.15	498.9	498
b'	562.65	564.25	564.15
b	819	821	819

Table 5. Exotherm peak temperatures, effect of rolling temperature in SiC_p A356 Al.

the same amount but at varying rolling temperatures; 400°C, 480°C and 545°C. Examination of Table 5 shows that differences between the β″ peak temperatures are not clearly discernible, but it appears that in general, the peak temperature decreases with decreasing rolling temperature; i.e., the β″ most accelerated is that for the sample rolled at 400°C. Additionally, the β″ exotherm is seen to become larger as rolling temperature is increased showing that the amount of β″ formed increases directly with rolling temperature.

From Table 5 it is also evident that the β′ peak of the MMC rolled at the highest temperature (545°C) is accelerated relative to the samples rolled at 480°C and 400°C. The latter two samples showed almost no β′ peak temperature variation between them. The volume fraction of β′ formed is seen to be the least for the MMC rolled at 545°C, while those rolled at 400°C and 480°C show nearly equal amounts of β′.

Figure 7 is the TEM micrograph for the MMC rolled to 24.6% reduction at 400 C and 10 % per rolling pass. This TMP schedule produced a recovered microstructure consisting of subgrains bounded by low angle boundaries. The dislocations within the subgrains boundaries were closely spaced. Overall, the dislocation density was moderate except for areas near SiC particles where dislocation density was generally heavier. Figure 5 is the TEM micrographs of the sample rolled to 27.6% reduction at 545°C and 10% per rolling pass. The features of this microstructure were detailed earlier.

The DSC thermograms in Figure 6 clearly shows that as rolling temperature increases, the volume fraction of β″ also increases. This suggests that the vacancy concentration in the sample strained to 27.6% at 545°C is higher than the sample strained to 24.6% at 400°C. As observed in the micrographs, the

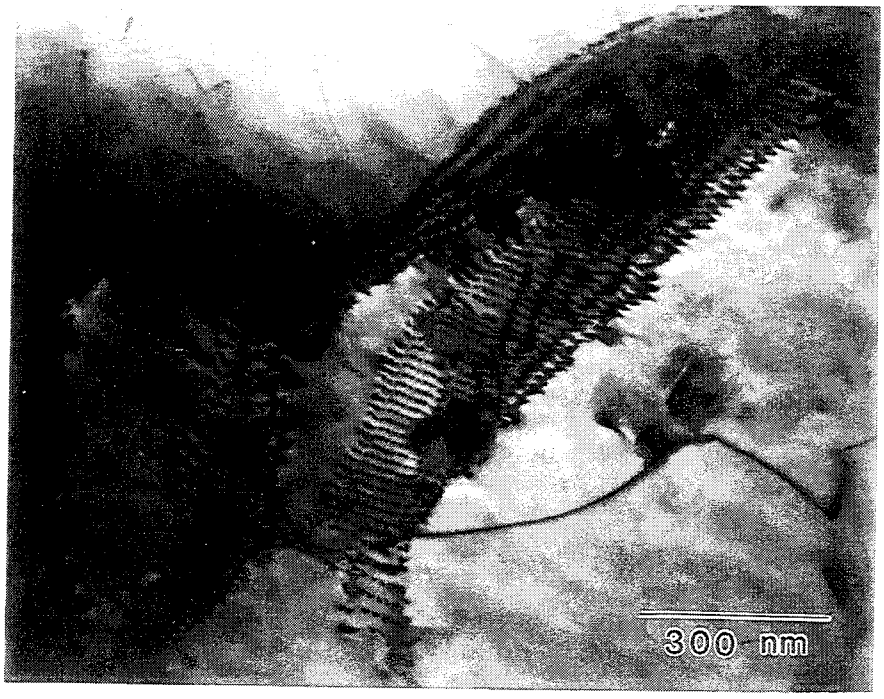

Figure 7. TEM micrograph of MMC rolled to 24.6% reduction at 400°C and 10% per rolling pass.

much higher dislocation density of the sample rolled at 400°C particularly in the areas around the SiC particles has had a more pronounced effect as a vacancy sink than the recrystallized structure of the sample rolled at 545°C with its lower dislocation density. The overall effect of a microstructure consisting of relatively high subgrain boundaries and low subgrain dislocation density, as in the 545°C sample, is to leave more quenched in vacancies than a microstructure consisting of subgrain boundary dislocations and a higher overall subgrain dislocation density, as in the 400°C sample. The higher vacancy concentration leads to increased β″ precipitation.

The competitive nature of the formation of β″ and β′ [Ref. 11] due to Mg depletion within the matrix suggests that the formation of a relatively large

amount of β″ phase will tend to result in relatively less β′ formation. This tendency is seen, to an extent, in Figure 6. The relative amounts of β″ and β′ formed between the MMC rolled at 545°C and the MMC rolled at 400°C exhibits the competitive nature of the formation of these two phases as the relative amounts are reversed on precipitating β′. However, the observation that both β″ and β′ peaks in the MMC strained at 480°C are larger than those in the MMC rolled at 545°C suggests that other factors need to be considered with regard to β′ precipitation.

It has been shown previously that dislocations are the preferred site for nucleation of the β′ phase. Once nucleated at random dislocations, the growth of β′ will depend on the diffusion of Mg remaining in solid solution either by dislocation pipes or by vacancy motion. Both modes compete for Mg and which one dominates could depend on the relative proportion of quenched-in vacancies in the matrix, and the density of random dislocations which serve as short circuit diffusion paths. The observation that more β′ precipitated in the MMC strained at 480°C than the MMC strained at 400°C suggests that an adequate dislocation density was available for β′ nucleation and that, relative to the 400°C MMC, the growth conditions via the relative proportion of dislocation pipes to vacancies favored growth of β′ in the 480°C MMC over β′ growth in the 400°C MMC.

D. EFFECT OF TOTAL ROLLING STRAIN

Figure 8 shows the DSC thermograms representing the effect of total rolling strain, 24.6% and 53% at 400°C, on the MMC as compared to the as cast MMC. Table 6 lists the peak temperatures observed in the same thermograms. From the peak temperature data it is seen that the β″ phase for the MMC strained to 24.6% at 400°C is slightly decelerated relative to the as-cast MMC and the MMC

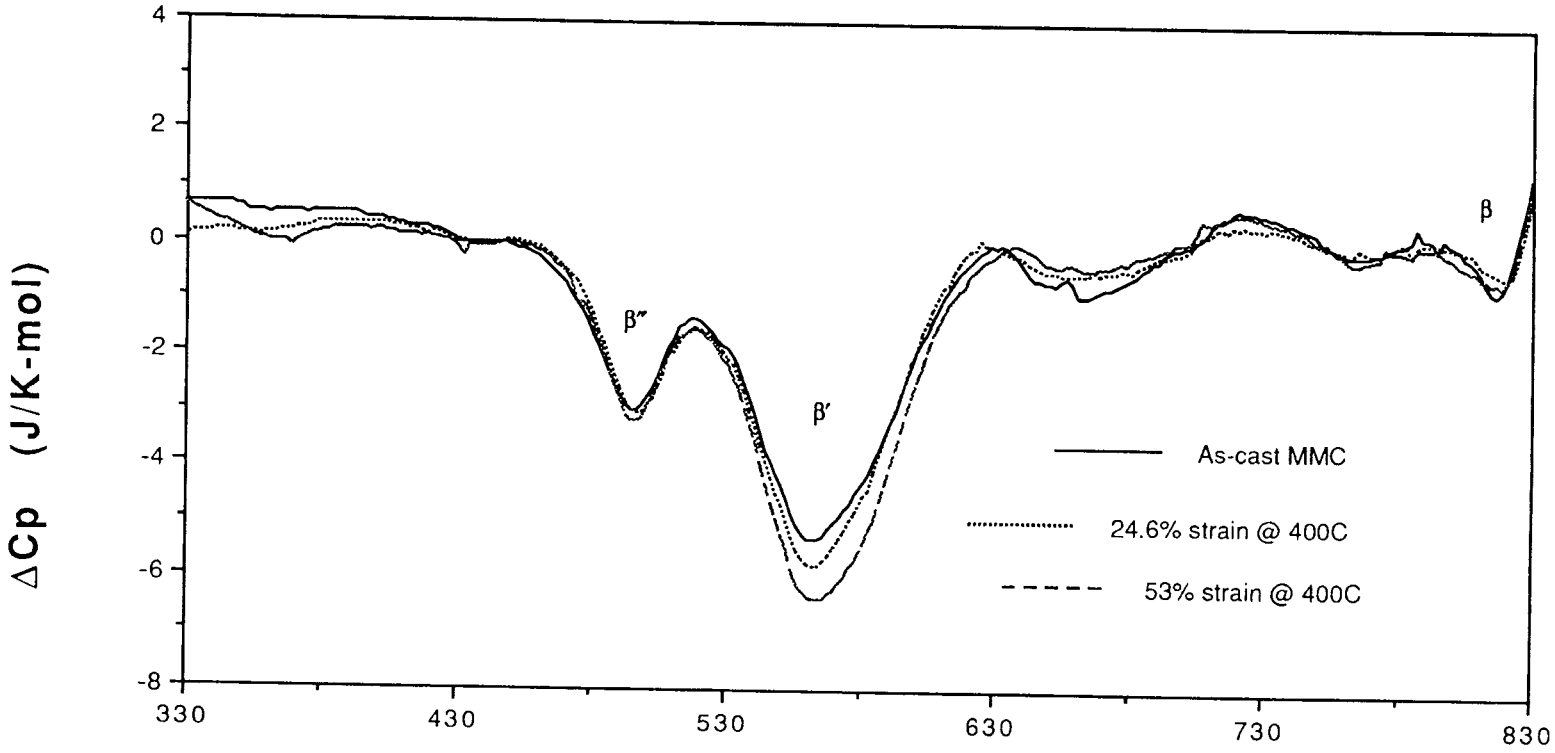

Figure 8. Effect of total rolling strain in SiC_p A356 Al at 400°C.

	As Cast MMC	24.6% @ 400C	53.5 @ 400C
Peak	Temp (K)	Temp (K)	Temp (K)
β"	496.35	498	495.7
β'	563.35	564.15	565.8
β	816	819	819

Table 6. Exotherm peak temperatures, effect of total rolling strain in SiC_p A356 Al at 400°C.

strained to 53% at 400°C. Further, the β′ peak, as a trend, is slightly decelerated with increasing strain. This deceleration with strain is consistent with results obtained by May [Ref. 12] in a study on the same material. Most notable in the thermograms of Figure 8 is the fairly constant amount of β″ precipitated in all three MMCs, followed by amounts of β′ that increases directly with strain.

TEM representation of the MMC strained to 53% at 400°C and 10 % per pass is shown in Figures 9(a) and 9(b). This TMP schedule produced a recovered microstructure consisting of subgrains bounded by low angle boundaries. Dislocations within the subgrain boundaries were clearly resolvable. In the areas adjacent to SiC particles dislocations were very dense as seen in Figure 9(a). Away from the particles, the dislocations density was moderate although notably more dense than the sample strained to 24.6% at the same temperature and strain per rolling pass.

As noted above, the β″ exotherms for all three MMCs are nearly identical. It was expected that the higher strain and resultant lower vacancy concentration due to absorption at dislocations would have a more pronounced effect on β″ precipitation kinetics and amounts. Given that the microstructures of these three samples are very similar with the exception of dislocation density, it is concluded that the difference between the dislocation densities in the three samples by themselves is not sufficient to affect the vacancy concentration enough to significantly influence β″ nucleation or Mg diffusion in the solid solution. Since β″ precipitates are very small, requiring only a very small fraction of the excess solute to come out of solution, the relatively small difference in vacancy concentration in the three samples (due to difference in the dislocation density) is not reflected in the β″ amounts.

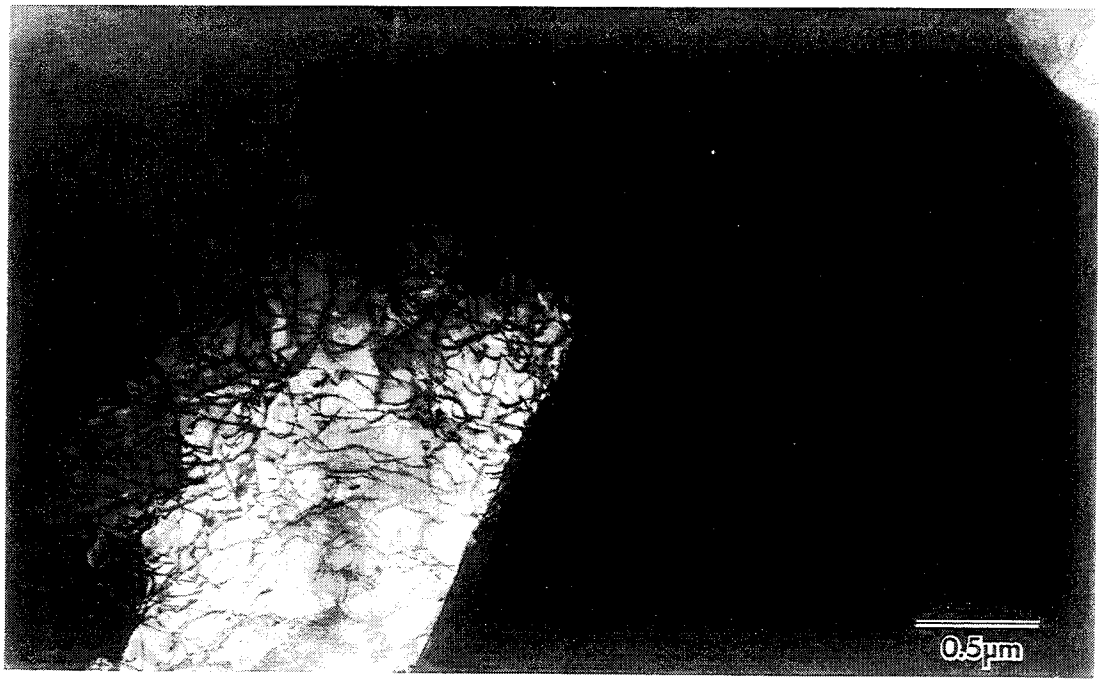

(a)

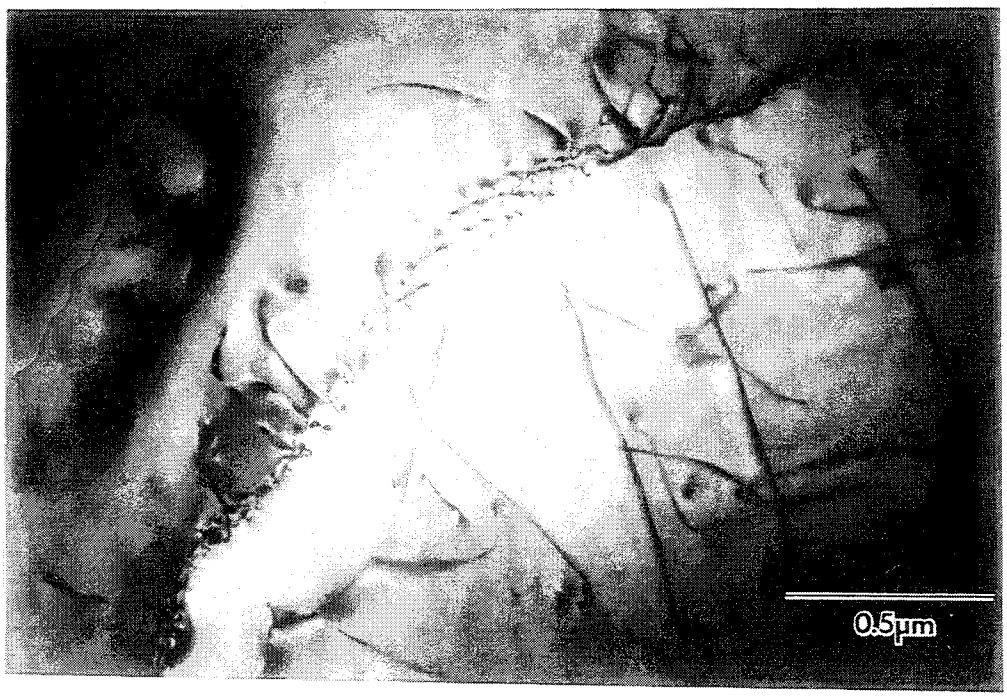

(b)

Figure 9. MMC strained to 53% at 400°C, 10% per rolling pass.

While not greatly affecting β″ precipitation, dislocation density shows a very pronounced effect on precipitation of β′. As dislocation density increases there is a proportionate increase in heterogeneous nucleation sites for β′ precipitation. Additionally, the dislocations enhance β′ growth by providing short circuit diffusion paths or dislocation pipes. As a result, β′ nucleation and growth is enhanced by the presence of dislocations resulting from hot working. Also noted from Figure 8, the rise in β′ volume fraction and subsequent depletion of solute from solid solution reduces the amounts of stable β precipitate.

The data presented here is consistent with results obtained by May [Ref. 12]. The addition of TMP to the material had the effect of decelerating the precipitation of both β″ and β′. However, TEM photomicrographs do not support the contention that recovery of interfacial dislocations to grain/subgrain boundaries has decreased the density of random dislocations available for precipitation within subgrains. Rather, it was observed under the TEM that random dislocation density in the MMC strained to 53% was higher than the MMC strained to 24.6%, both rolled at 400 C. It is plausible that the additional strain in the metal matrix increases the energy barrier, ΔG^*, for nucleation due to an increased strain energy term, ΔG_ε. Once this energy barrier is overcome, growth is aided by short circuited diffusion paths.

(blank)

VI. CONCLUSIONS

The addition of ceramic particulates has a pronounced effect on aging kinetics of the as cast A356 aluminum alloy. In comparison to the monolithic alloy, the β″ and β′ phases are both accelerated by the addition of SiC particulate to the aluminum matrix with the β′ phase showing the most significant degree of acceleration. Further, the amount of precipitates is affected by the addition of SiC_p. The amount of β″ formed in the as cast MMC is increased whereas the amount of β′ phase is reduced.

Thermomechanical processing of the as-cast MMC had no significant impact on aging kinetics of the matrix alloy. This would suggest that the addition of SiC_p has a much stronger effect on matrix precipitation (and hence on the matrix vacancy concentration and dislocation density which provide sites for nucleation and affect growth) than post-fabrication thermomechanical processing, at least within the strain and temperature ranges examined here.

From the TEM investigation, it was found that the addition of 24.6% strain by rolling at 400°C induces a recovered microstructure with a well defined sub-cell structure consisting of low angle boundaries. Increasing rolling strain to 53% primarily affected only the dislocation density by increasing it notably. Varying the strain per pass while rolling to 27% reduction at 545°C affected subgrain boundary misorientation significantly, as seen under the TEM. Straining at 5% per pass resulted in a recovered microstructure whereas 10% per pass resulted in a nearly recrystallized microstructure.

The effect of increasing rolling temperature while holding rolling strain constant slightly decelerated the formation of the β″ metastable phase while also

increasing the amount of β″ formed. The transformation kinetics of the β′ phase was not affected by rolling temperature, but the amount of β′ formed decreased with increasing rolling temperature.

Increasing the amount of total rolling strain at 400°C had a trivial effect on the precipitation kinetics and growth of β″ metastable phase. Precipitation of the β′ phase was slightly decelerated with increased rolling strain, consistent with results obtained by May [Ref. 12]. Most notably, there was a marked increase in β′ precipitation with matrix strain.

At 545°C, increasing the strain rate from 5% per rolling pass to 10% per rolling pass had little effect on aging kinetics of A356 MMC. The amounts of β″ and β′ increased slightly with increased strain per pass.

Finally, it is concluded that a TMP schedule that resulted in an observable increase in dislocation density also resulted in an increase in β′ transition phase.

REFERENCES

1. Karmarkar, S.D., Divecha, A.P., *Centrifugal Casting of Composites*, United States Patent Number: 5,025,849, June 25,1991.

2. Martense, A., Cornie, J.A., and Flemings, M.C., "Solidification Processing of Metal Matrix Composites", *Journal of Metals*, pp.12-19, vol.40, no.2, February 1988.

3. Girot, F.A., Albringre, L., Quenisset, J.M., and Naslain, R., "Rheocasting Al Matrix Composites:, *Journal of Metals*, pp. 18-21, vol. 39, No.11, November 1987.

4. Cottu, J.P., Couderc, J.J., Viguier, B., Bernard, L., "Influence of SiC reinforcement on Precipitation and Hardening of a Metal Matrix Composite", *Jounal of Materials Science*, pp. 3068-3074, vol. 24, June 1992.

5. Samual, A.M., "Effect of Melt, Solidification and Heat treatment of Al-Si-Mg/SiC_p Alloy", *Journal Materials Science*, vol.23, pp. 6785-6798, December, 1993.

6. McNelley, T.R., and Kalu, P.N., "The Effects of Thermomechanical Processing on the Ambient Temperature Properties and Aging Response of 6061 Al-Al_2O_3 Composit", *Scripta Metallurgica*, vol25, pp. 1041-1046, 1991.

7. Kalu, P.N., and Mcnelley, T.R., "Microstructural Refinement by Thermomechanical Treatment of a Cast and Extruded 6061 Al-Al_2O_3 Composite", *Scripta Metallurgica*, vol. 25,pp. 853-858, 1991.

8. Samual, A.M., Samual, F.H., "Influence of Casting and Heat Treatment Parameters in Controlling the Properties of an Al-10wt% Si-0.6wt% Mg/$SiC/20_p$ Composite", *Journal of Materials Science*, vol. 29, pp. 3591-3600, July, 1994.

9. Das, T., Bandyupadhyay, S., Blairs,S., "DSC and DMA Studies of Particulate Reinforced Metal Matrix Composites", *Journal of Materials Science*, vol. 29, pp. 5680-5688, March 1994.

10. Hadianfard, M.J., Yiu-Wing Mai, Healy, J.C., "Effect of Ceramic Reinforcement on the Aging Behaviour of an Aluminium Alloy",*Journal of Material Science*, vol. 23, pp. 3665-3669, July 1993.

11. Dutta, I., Allen, S.M., Hafley, J.L., "Effect of Reinforcement on the Aging Response of Cast 6061 Al-Al_5O_3 Particulate Composites", *Metallurgical Transactions A*, vol. 22A, pp. 2553-2563, November 1991.

12. May, C.M., "Effect of Thermomechanical Treatments on the Aging Response of Centrifugally Cast Silicon Carbide/Aluminum Composites", Master's Thesis, Naval Postgraduate School, Monterey, Calofornia, September 1991.

13. Thomas, M.P., King, J.E., "Comparison of the Aging Behaviour of PM 2124 Al Alloy and Al-SiC_p Metal-Matrix Composite", *Journal Material Science*, vol. 29, pp. 5272-5278, April 1994.

14. Garcia-Cordovilla, C., Louis, E., Narciso, J., Pamies, A., "A Differential Scanning Calorimetry Study of Solid State Reactions in AA6061-SiC, AA6061-Al_2O_3 and A357-SiC Composites Fabricated by Means of Compocasting", *Materials Science and Engineering*, March 1994.

15. Dutta, I., Harper, C.P., Dutta, G., "Role of Al_2O_3 Particulate Reinforcement on Precipitation in 2014 Al-Matrix Composites", *Metallurgical and Materials Transactions*, vol. 24A, pp. 1591-1602, August 1994.

16. Dutta, I., Allen, S.M., "A Calorimetric Study of Precipitation in Commercial Aluminum Alloy 6061", *Journal of Materials Science Letters*, vol. 10, pp. 323-326, 1991.

17. *Metals Handbook*, 10th Edition, vol. 2, ASM International, 1990.

18. Dutta, I., Tiedemann, C. F., and McNelley, T.R., "Effect of Hot Working on the Microstructure and Porperties of a Cast Al-SiC_p Metal Matrix Composite", *Scripta Metallurgica*, vol. 24, no. 4, pp. 1233 - 1235, 1990.

19. Porter, D.A., Easterling, K.E., *Phase Transformations in Metals and Alloys*, pp. 263-287, T.J. Press Ltd., Padstow, Cornwall, 1987.

20. Muller, K.A., "Effect of Post-Fabrication Processing on the Tensile Properties of Centrifugally Cast SiC Particulate Reinforced Alumium Composites", Master's Thesis, Naval Postgraduate School, Monterey, California, September 1993.

21. McNelley, T.R., Crooks, R., Kalu, P.N., and Rogers, S.A., "Precipitation and Recrystallization During Processing of a Superplastic Al-10Mg-0.1Zr alloy", *Materials Science and Engineering*, pp. 135-143, 1993.

INITIAL DISTRIBUTION LIST

		No. Copies
1.	Defense Technical Information Center Cameron Station Alexandria, Virginia 22304-6145	2
2.	Library, Code 52 Naval Postgraduate School Monterey, California 93943-5101	2
3.	Naval/Mechanical Engineering Curricular Office (Code 34) Naval Postgraduate School Monterey, California 93943-5100	1
4.	Professor I. Dutta, Code ME/Du Naval Postgraduate School Monterey, California 93943-5000	1
5.	Dr. S. D. Karmarkar Code R32 Naval Surface Warfare Center, White Oak Silver Spring, MD 20903	1
6.	Dr. A.P. Divecha Code R32 Naval Surface Warfare Center, White Oak Silver Spring, MD 20903	1
7.	Donald V. Avenger 627 S. Nixon Lima, OH 45805	1